Available online at www.sciencedirect.com
SCIENCE DIRECT
Thin Solid Films 506–507 (2006) 559 – 563
thin solid films
www.elsevier.com/locate/tsf

Plasma performance in very large helicon device

T. Tanikawa [a,*], S. Shinohara [b]

[a] Research Institute of Science and Technology, Tokai University, 1117 Kitakaname, Hiratsuka, Kanagawa 259-1292, Japan
[b] Interdisciplinary Graduate School of Engineering Sciences, Kyushu University, 6-1 Kasuga Koen, Kasuga, Fukuoka 816-8580, Japan

Available online 12 September 2005

Abstract

A large volume (75 cm in diameter and 486 cm in axial length) helicon-plasma device has been developed, and the plasma characteristics in the device have been investigated. With the use of a large (43 cm in outer diameter) spiral antenna located just outside a quartz-glass window at the end of the vacuum chamber, the device is capable of producing high-density plasma (gas species used so far are argon (Ar) and helium (He)) of $n_e \geq 10^{12}$ cm^{-3} with moderate rf input power of less than 1 kW, showing excellent discharge efficiency. With this device it is possible to control the radial density profile employing the following two techniques: (1) changing the magnetic-field configuration near the antenna and (2) changing the antenna radiation-field patterns.

Keywords: Helicon plasma source; Profile control; Spiral antenna; Large-volume high-density plasma

1. Introduction

The development of a large volume plasma source capable of producing high-density plasma is very important in various plasma applications, such as in plasma processing, magnetic confinement fusion, and space plasma simulations, to name a few. Having ways to freely adjust the plasma density profile under various magnetic-field configurations is also a much desired feature in these applications. A helicon plasma source [1–5] that employs helicon waves for plasma production has been extensively investigated because of its efficient plasma production capability and can be a good candidate to achieve the above mentioned goals.

We have recently developed a high-density helicon plasma source with a large volume, 75 cm in diameter and 486 cm in axial length, at the Institute of Space and Astronautical Science, the division of the Japan Aerospace Exploration Agency, (ISAS/JAXA), and the plasma characteristics in the device have been extensively investigated. For this device, we have employed a spiral antenna scheme, aiming to produce a large volume helicon plasma with high efficiency and further to control the radial density profile utilizing the following two techniques: (1) changing the magnetic field configuration near the spiral antenna and (2) changing the antenna radiation-field patterns. Developing easy ways to control the density profile is crucial in many plasma applications. Therefore, our large plasma source with the capability of controlling the plasma density profile can contribute to extending opportunities for plasma processing with a large-diameter, high-density plasma under low fill-pressure conditions.

In this paper, we present the main features of our large-volume helicon plasma device. In order to further improve the plasma performance, lines of permanent magnets have been installed around the plasma column in front of the antenna and the downstream end of the chamber (see Fig. 1). The magnets are arranged in such a way that they can produce a multi-mirror surface field [6]; as a result, ionizing primary electrons can be better confined in the device so as to enhance the plasma production efficiency. The effect of installing permanent magnets to the plasma performance will be briefly described.

2. Experimental setup

Fig. 1 is a schematic of our large-volume helicon plasma device at ISAS/JAXA. A detailed description of the device

* Corresponding author.
E-mail address: tnth@keyaki.cc.u-tokai.ac.jp (T. Tanikawa).

0040-6090/$ - see front matter © 2005 Elsevier B.V. All rights reserved.
doi:10.1016/j.tsf.2005.08.053

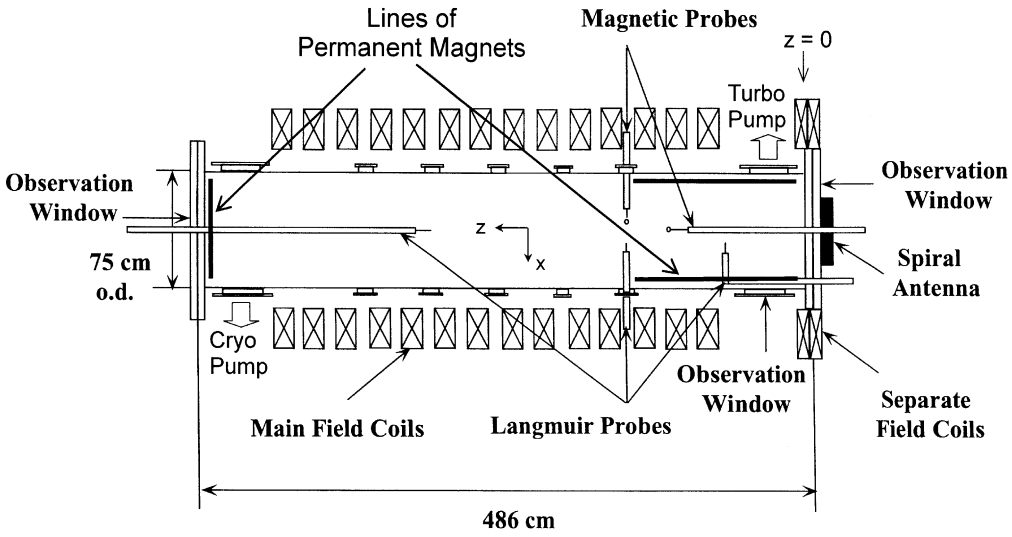

Fig. 1. Schematic of the large-volume, helicon plasma device at ISAS/JAXA.

including the rf system can be found in Ref. [7]. The dimensions of the vacuum chamber are: 75 cm and 73.8 cm in outer diameter (o.d.) and inner diameter (i.d.), respectively, and 486 cm in axial length. Fourteen main coils produce a uniform magnetic field in the central region of over 2 m extent along the axial direction (see Fig. 2), where the main coil current of I_m=50 A generates the field strength of 140 G. Due to the lack of coils at both ends of the device, the magnetic field in these regions becomes weaker and nonuniform. In order to compensate for the weak magnetic field near the spiral antenna located at one end of the chamber, additional field coils (Separate Field Coils in Fig. 1) are installed; an independent power supply is used to energize them. Here, the three different values of the separate coil current, I_s=0, 10 and 20 A, correspond to the axial magnetic field near the antenna B_a=11, 30 and 50 G, respectively, with I_m=50 A, as shown in Fig. 2. We note that varying I_s does not significantly alter the strength of the main magnetic field B_m in the central region of the chamber that is mostly generated by I_m. It can be seen from Fig. 2(a) to Fig. 2(c) that increasing I_s makes the degree of divergence of the field near the z=0 region weaker. Here, the position z=0 corresponds to the inner surface (vacuum side) of the quartz-glass window for the antenna. As will be described in Section 3.2, it is possible to control the radial density profile of plasma by changing the magnetic field profile near the antenna (through varying I_s).

A photograph of the large spiral antenna (4 turns with 43 cm o.d.) is shown in Fig. 3. The antenna has metal taps for electrical connections at every half-spiral turn. Any two connection points can be chosen to feed the rf power to the antenna; in this way the antenna radiation-field pattern can be varied quite easily. This provides another way to control the radial density profile as will be presented in Section 3.2. The antenna is installed just outside the vacuum vessel in

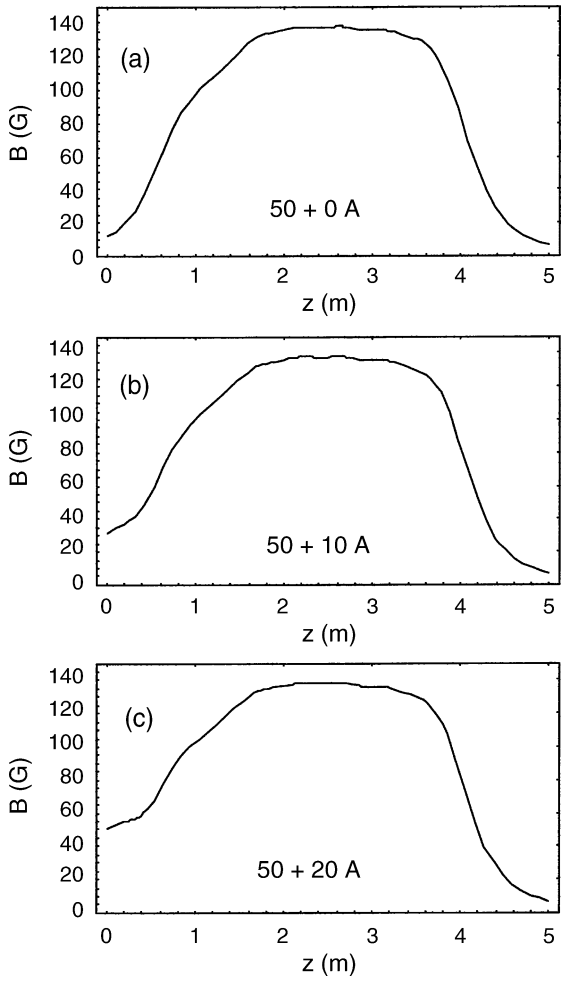

Fig. 2. Calculated axial profiles of the magnetic field for three different values of the separate coil current I_s near the antenna. The strength of the main field is 140 G (the main coil current I_m=50 A). (a) I_s=0 A, (b) I_s=10 A, and (c) I_s=20 A.

Fig. 3. Large diameter (43 cm o.d.) spiral antenna.

atmosphere through a quartz-glass window (52 cm in diameter and 3 cm in thickness). The rf frequency used to produce plasma is 7 MHz. Plasma is usually produced repetitively with the rf discharge-pulse duration of 40 ms and the pulse interval of 1 s. The working gas species used are Ar (0.1–2 mTorr) and He (0.2–1 mTorr).

Permanent magnets (the field strength at the surface is 1 kG) are encased in long air-tight, stainless-steel boxes; then, they are mounted on two stainless-steel cylindrical frames so as to form a multi-mirror surface field inside the cylinders [6]. We call these cylindrical frames with permanent magnets "magnet cages". The inner diameter of the magnet cages is 63.8 cm. The length of one of them is 67.5 cm and that of the other is 60.5 cm. They are placed inside the vacuum vessel toward the quartz-glass window (see Lines of Permanent Magnets in the right-hand side of Fig. 1). The first cage is placed between $z=19$ cm and 86.5 cm, while the second one is placed between $z=87.5$ cm and 148 cm. Note that the two magnet cages are shown as thick bars in Fig. 1. Lines of permanent magnets that form a multi-mirror surface field are also installed on the end-flange as shown in Fig. 1.

The spatial plasma parameters, such as the electron density n_e and the electron temperature T_e (typically 3–5 eV), are measured by spatially scanning Langmuir probes. The excited rf wave field patterns are measured using one-turn magnetic probes.

3. Experimental results and discussion

3.1. Basic characteristics of plasma

The electron plasma density n_e is plotted against the input rf power, P_{inp}, at two different axial locations without installing the primary electron confining magnet cages (i.e., without having Lines of Permanent Magnets in Fig. 1) in Fig. 4(a) and after installing them in Fig. 4(b), respectively. Plasma production can be initiated at as low as $P_{inp} \leq 1$ W, where n_e is on the order of 10^9 cm^{-3}. The discharge mechanism in this low-density regime can be categorized as a capacitively coupled plasma (CCP) discharge. In this regime of $n_e < 10^{10}$ cm^{-3}, the antenna loading is several times worse than that in the high density regime of $n_e \approx 10^{12}$ cm^{-3}. As P_{inp} is increased, the plasma behavior alters from a CCP to a helicon plasma (HP) discharge through the regime of an inductively coupled plasma (ICP) discharge. When P_{inp} exceeds the threshold power P_{th}, the density jump to $n_e \leq 10^{12}$ cm^{-3} occurs. This jump is characterized by a steep increase in n_e (sometimes exceeding one order of magnitude in increase) accompanied by the mode transition from an ICP to a HP discharge. We note that wave propagation along the z-axis is not observed before the density jump. Wave dispersion measurements (made by using axially and radially movable one-turn magnetic probes) after the density jump have indicated that wave characteristics are consistent with those

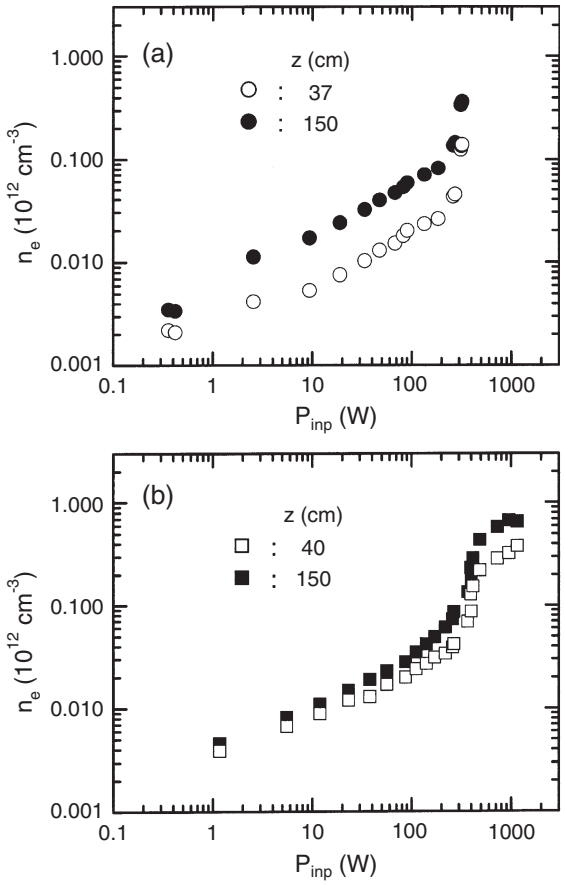

Fig. 4. Relationship between the electron density n_e and the input rf power P_{inp} for Ar plasma ($p_{Ar}=0.5$ mTorr). (a): without installing the magnet cages (i.e., without Lines of Permanent Magnets in Fig. 1). (b): the magnet cages installed. The main magnetic field strength is 140 G ($I_m=50$ A) and $I_s=16$ A. Full 4 turns of the spiral antenna are used and a high-voltage feed-point is at the center of the antenna. For (a), $P_{th} \approx 250$ W, while $P_{th} \approx 390$ W for (b).

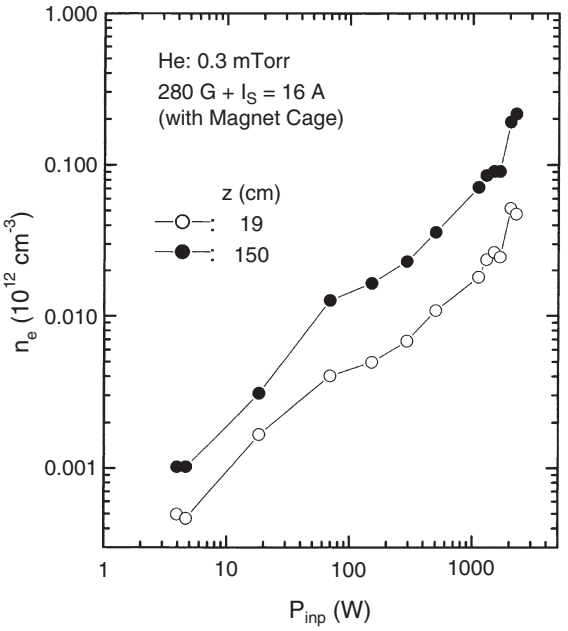

Fig. 5. Relationship between the electron density n_e and the input rf power P_{inp} for He plasma (p_{He}=0.3 mTorr). The magnet cages (Lines of Permanent Magnets in Fig. 1) are installed for the measurements. The main magnetic field strength is 280 G (I_m=100 A) and I_s=16 A. Outer 2 turns of the spiral antenna are used and a high-voltage feed-point is at the outer most position of the antenna. $P_{th} \approx 2000$ W.

of the m (azimuthal mode number)=0 helicon wave, confirming a HP discharge after the jump. The radial profile of the axial component of the rf magnetic field can be fitted to the Bessel function of J_0, showing also the m=0 helicon wave characteristic. The value of P_{th} and the magnitude of the density jump, Δn_e, increase as the separate coil current I_s (or the magnetic field strength near the antenna) is raised. We have found that the wave structure after the jump tends to be clearer with the increase in I_s. After the jump, the plasma density gradually increases as P_{inp} is raised. The saturation of the plasma density is not observed up to the available maximum rf power (~2 kW) in our experiments.

When the permanent magnet cages (Lines of Permanent Magnets in Fig. 1) are installed, P_{th} becomes higher than the case without the magnet cages. At the same time, the axial uniformity of the plasma improves. This is reflected in the closer values of n_e between two different axial positions in Fig. 4(b). With the magnet cages, starting a discharge is somehow easier than in the case without the magnet cages. For example, starting a discharge with helium gas is rather difficult. For the condition of Fig. 5, one would need an external electron source, such as a small electron emitting filament, in order to initiate a discharge, if the magnet cages were not installed. Then, repetitive discharges would not be able to be sustained without electron sources. However, with the magnet cages near the antenna and the lines of permanent magnets at the end of the chamber, no external electron source is necessary to sustain plasma.

3.2. Control of radial density profile

For this part of the experiment, no primary electron confining magnet cages, or lines of permanent magnets, are installed inside the chamber (there is one exception in Fig. 7).

The first method to control the radial density profile involves changing the magnetic field configuration near the antenna. It can be easily achieved by varying the separate coil current, I_s. With a higher value of I_s, the curvature of converging field lines becomes gentler, resulting in a smoother flow of plasma to the uniform field region. This makes the plasma-column diameter larger.

The second method to control the radial density profile utilizes the different patterns of the antenna radiation field. We are able to vary the radial density profile by changing the rf feed points on the antenna. The cases studied are:

(1) Full 4 turns: The rf feed-points are the antenna center and the outer most position. If the high-voltage side of the rf amplifier is connected to the center, it is indicated as “Inner HV”, while the opposite case is “Outer HV”.
(2) Outer 2 turns: The rf feed-points are the outer most position and the second spiral position. There are two cases depending upon which side is connected to the HV side of the amplifier.
(3) Inner 2 turns: The rf feed-points are the center and the second spiral position. There are two possible HV connections.

Various combinations of I_s and the antenna connections can be tried to obtain an optimal profile for a particular purpose. Some examples are shown in Figs. 6 and 7. The widest plasma column diameter is basically determined by

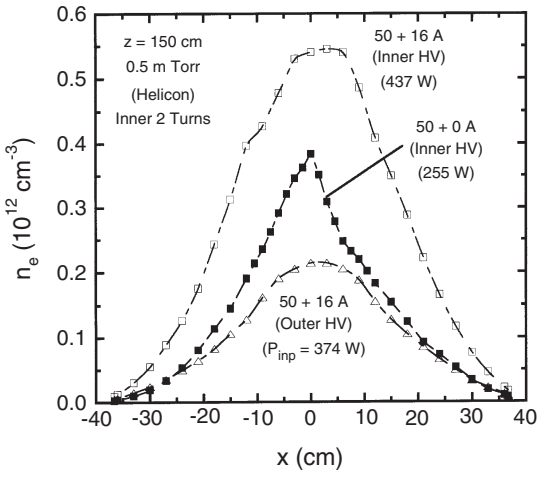

Fig. 6. Radial profiles of the electron density n_e at z=150 cm for Ar plasma (p_{Ar}=0.5 mTorr). The main magnetic field strength is 140 G (I_m=50 A). Inner 2 turns of the spiral antenna are used. A high-voltage feeding point and the value of I_s are varied. All three profiles are measured after the density jump.

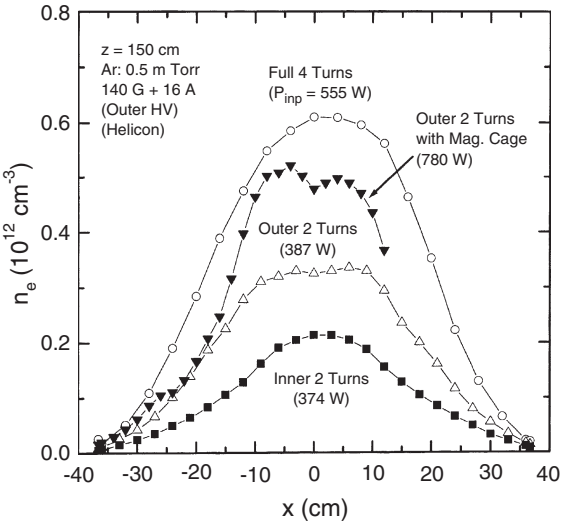

Fig. 7. Radial profiles of the electron density n_e at $z=150$ cm for Ar plasma ($p_{Ar}=0.5$ mTorr). The main magnetic field strength is 140 G ($I_m=50$ A) and $I_s=16$ A. A high-voltage feeding point is fixed at the outer most position of the antenna. All four profiles are measured after the density jump.

the antenna diameter. Obtaining a flatter profile seems to be more difficult than obtaining a peaky profile. For a plasma in the HP mode, it appears that the best way to obtain a flatter radial density profile is to use the outer 2 turns of the antenna with the outer HV connection and to have a more uniform magnetic-field near the antenna (i.e., the larger I_s).

4. Conclusions

A high-density helicon plasma source with a large volume, 75 cm in diameter and 486 cm in axial length, has been developed and the plasma characteristics in the device have been investigated in detail, demonstrating highly efficient plasma production. With this device, it is possible to control the radial density profile by using the following two techniques: (1) changing the degree of nonuniformity of the magnetic field near the antenna by adjusting the separate field coil current I_s and (2) changing the antenna radiation-field pattern by using different rf feeding points on the spiral antenna. It appears to be advantageous to use the outer 2 turns of the 4-turn spiral antenna with the outer HV connection in order to have a flatter radial density profile for a helicon plasma. Having a more uniform magnetic field near the antenna is also preferable.

It has been found that magnet cages in the antenna side of the chamber can help improve the plasma performance by prolonging the confinement of ionizing primary electrons and by partially compensating the weak field near the antenna.

Acknowledgments

Our experiments were carried out at ISAS/JAXA under their research collaboration program. Encouragement from Professor Y. Nakamura, Professor Y. Kawai, Professor K. Oyama, and Professor K. Toki is greatly appreciated. We would also like to thank Dr. S. Sato, Dr. I. Funaki, and Mr. K. Aihara for their assistance in carrying out the experiments. The research was partially supported by the Grants-in-Aid for Scientific Research (B)(2) the contract #15340199 and #1435051 from the Japan Society for the Promotion of Science.

References

[1] R.W. Boswell, Phys. Lett. 33A (1970) 457.
[2] M.A. Lieberman, A.J. Lichtenberg, Principles of Plasma Discharges and Materials Processing, John Wiley & Sons, New York, 1994, p. 434.
[3] S. Shinohara, Jpn. J. Appl. Phys. 36 (1997) 4695 (and references therein).
[4] R.W. Boswell, F.F. Chen, IEEE Trans. Plasma Sci. 25 (1997) 1229 (and references therein).
[5] F.F. Chen, R.W. Boswell, IEEE Trans. Plasma Sci. 25 (1997) 1245 (and references therein).
[6] K.N. Leung, N. Hershkowitz, K.R. MacKenzie, Phys. Fluids 19 (1976) 1045.
[7] S. Shinohara, T. Tanikawa, Rev. Sci. Instrum. 75 (2004) 1941; Phys. Plasmas 12 (2005) 044502.